TURBULENCE AND DIFFUSION NOTES NO 26

THE DEVELOPMENT OF A DRY INVERSION-CAPPED CONVECTIVELY UNSTABLE BOUNDARY LAYER

by

D J CARSON

AUGUST 1972

Boundary Layer Research Branch
Met O 14
Meteorological Office
Bracknell

SUMMARY

A model is proposed for the development of a dry convectively unstable boundary layer capped by a stable layer ; included are the effects of time-dependent surface heating, the stability of the capping layer, subsidence and any degree of turbulent interfacial mixing. A differential equation describing the evolution indicates quantitatively the relative importance of each factor and, in particular, indicates the importance of the entrainment process. The model is applied to the 1953 O'Neill boundary layer data in an attempt to assess to what degree interfacial mixing is realised in the atmosphere. Realistic boundary layer developments are obtained.

1. INTRODUCTION

A principal aim of boundary layer study is to identify the characteristics necessary to determine the energy exchanges between the free atmosphere and the Earth's surface, so that methods can be devised for incorporating these important effects in numerical forecasting and general circulation models. Basically the problem has three stages:

(i) Estimation of the appropriate heat, moisture and momentum fluxes which enter the boundary layer from the Earth's surface,

(ii) Distribution of the fluxes within the boundary layer,

(iii) Control of the exchanges between the boundary layer and the free atmosphere.

Current boundary layer techniques provide only a first approximation to the important surface fluxes and this problem still demands much more consideration. The remaining stages raise the question of the suitability of employing schemes which imply a fixed depth of boundary layer allowing an almost continuous exchange of heat and moisture with the free atmosphere through diffusion processes coupled with convective adjustment mechanisms when the lowest layers become unstable relative to each other. The boundary layer is not stationary but, in some important cases, is a diurnally evolving system with discontinuities. Fluxes entering the layer control its development but do not substantially effect the free atmosphere (except through entrainment into the boundary layer) until marked energy transfer is induced by boundary layer breakdown or stabilization due, for example, to advection, deep convection or generally disturbed frontal weather conditions.

A scheme for inserting the boundary layer's intrinsic evolutionary nature into large scale models was proposed by Charnock and Ellison (1967) who, from a study of radio-sonde ascents over the NE Atlantic, classified the boundary layer into a small number of different types and observed that the dry convectively unstable boundary layer capped by a deep non-turbulent stable layer accounted for about fifty per cent of the available cases. Several salient points were re-emphasized by Charnock (1972). The scheme, discussed and modified by Smith (1968), assumes the existence of a definable interface, h, between the convectively unstable and the quiescent stable layers. The importance of the spatial and temporal variations of h when parameterizing the boundary layer for use in general circulation models is emphasized in a comprehensive study by Deardorff (1972 a) which provides an alternative approach to those proposed by Clarke (1970 a, b) and Delsol, Miyakoda and Clarke (1971) in which several fixed layers in the first few kilometres are used to resolve the boundary layer's vertical structure and the distribution of the fluxes.

A realistic knowledge of the depth of the boundary layer is also important in other spheres. A practical method for estimating, and indeed forecasting, the depth is required, for example, in schemes for estimating the dispersion of concentrations of atmospheric pollutants and was the motivation of Hanna's (1969) investigation of several methods currently available for estimating the thickness of the steady boundary layer. Examination of Hanna's results emphasizes that formulae established for steady, neutral conditions are totally inadequate when dealing with the developing, diabatic boundary layer.

There is then a real need to investigate and understand the physical and dynamical processes which govern the evolving and spatially varying boundary

layer and a start would be to consider the development of the important dry, inversion-capped, convectively unstable layer. The first specific theoretical study of this situation was due to Ball (1960, 1962) who discussed the two main factors controlling the growth of the convective layer, namely,

(i) the flux of sensible heat into the layer from the strongly heated surface,

(ii) the mixing process at the unstable-stable interface level, h, the top of the boundary layer.

Ball's theoretical results and those of subsequent workers, notably Lilly (1968) and Deardorff, Willis and Lilly (1969) (see for example the review by Plate (1971)) rely on restrictive assumptions about the nature of the turbulent mixing at h and leave two important questions unanswered :

(i) How important is <u>any</u> degree of turbulent interfacial mixing to the rate of entrainment of the stable layer into the convectively unstable boundary layer.

(ii) To what degree is interfacial mixing realised in the atmosphere during the typical development of a convectively unstable boundary layer.

The aim of the present study is to provide a simple, but realistic, model describing such a developing boundary layer, including the effects of a continuous, time-dependent, surface sensible heat flux, a synoptic scale vertical velocity field (generally taken to be a subsidence field), the gradient of potential temperature in the stable layer and, most importantly, the effect of sensible heat brought into the layer through mixing at the interface, h. The results indicate the relative importance of each of the above parameters and provide an answer to question (i). The second question cannot be answered using

the model but application to the 1953 O'Neill boundary layer observations (Lettau and Davidson, 1957) suggests several distinct phases in the convectively unstable boundary layer's evolution.

2. THE DIURNAL VARIATION OF THE BOUNDARY LAYER DEPTH

Figure 1, derived and discussed in an earlier study by Carson (1971), illustrates the diurnal variation of the mean boundary layer thickness, $\langle h(t) \rangle$, and the surface sensible heat flux, $\langle H(0,t) \rangle$, observed in strongly convective daytime conditions in August-September, 1953 over the flat prairies at O'Neill. Lettau's estimated heat fluxes were used and although the absolute magnitudes may be significantly in error, the relative magnitudes and hence the diurnal pattern are thought to be realistic. $\langle H(0,t) \rangle$ is small, negative and effectively steady throughout the night-time period but after changing sign about an hour after sunrise varies markedly, almost sinusoidally, with a maximum value close to midday, before changing sign again about an hour and a half before sunset.

From the discontinuities in $\langle h(t) \rangle$ in the neighbourhoods of sunrise and sunset we distinguish between the relatively shallow night-time inversion layer in which buoyancy and viscous effects suppress any mechanically generated turbulent motions and the eventually deeper, daytime, well-mixed layer. The evolution of the nocturnal boundary layer, although not so pronounced as that of the daytime convectively unstable layer, is nontheless very important in pollutant dispersal problems and has been studied by Deardorff (1972 b). Although the vertical resolution of the O'Neill profiles is not suitable for detailed analysis of the nocturnal boundary layer thickness we note the typical growth of $\langle h(t) \rangle$ from near sunset to just after sunrise.

Our study is restricted to the unstable phase of the diurnal evolution. As $\langle H(0,t) \rangle$ becomes positive and begins to increase shortly after sunrise so the unstable layer begins to develop and the nocturnally established inversion is gradually eroded from below. This achieved, the highly turbulent boundary layer, driven by the increasing incoming radiation received at the surface, will, for a period, deepen at an enhanced rate. There follows a phase when the depth of the boundary layer remains steady or even begins to decrease and finally, when the surface sensible heat flux becomes negative, the nocturnal layer re-establishes itself from the surface. This is the type of evolution which a model must be capable of describing. For detailed qualitative descriptions of the convectively unstable boundary layer's development see, for example, Ball (1960) and Plate (1971).

It is worth noting that Hanna (1969) tested steady state (and in some cases neutral) formulae against the O'Neill data and their inability to account for the evolutionary nature of the situation is undoubtedly a major reason for the large scatter obtained in his comparisons of theoretically derived against profile-estimated depths of the boundary layer. Following Hanna, a preliminary study of the same data by Carson (1971) showed that formulations based on steady state similarity theory, e.g.

$$h = \frac{u_*}{f} S(\mu)$$

where $\mu = \frac{k u_*}{f L}$ is a stability parameter,

u_* is the surface friction velocity, L the surface layer Monin-Obukhov length, f the coriolis parameter, k the von Karman constant and S is a function of μ ,

are totally inadequate and that time dependent models are essential. The same conclusion was stated by Deardorff (1972b) when discussing the growth rate of the nocturnal boundary layer.

3. A SIMPLE MODEL

Figure 2 gives a schematic representation of the adopted typical potential temperature, θ , profile in a developing convectively unstable boundary layer. The shallow superadiabatic layer ($\leq$ few tens of metres) with its large vertical shears of wind and temperature is assumed to incorporate the regions of forced and mixed convection (Townsend (1962), Deardorff and Willis (1967)) where heat is predominantly transported by mechanically induced turbulent motions. We take this layer as the surface layer where flux-gradient or Jacobs-type formulae could be applied to give estimates of the surface fluxes; henceforth it is neglected. The thorough turbulent mixing in the free convection layer above the surface layer is buoyancy dominated and is assumed to produce a θ-profile virtually independent of height (Webb, 1958), although it is often observed to be slightly stable, particularly in the upper region of the layer.

The laboratory experiments of Deardorff, Willis and Lilly (1969) show the unstable-stable interface to be a highly contorted, almost undefinable surface due to the physical overshooting into the stable layer of energetic convective elements which originate in the surface layers and continually bombard the interface. Within this strongly agitated region the temperature field indicates marked spatial, perhaps discontinuous, variability, the net effect being a change across the layer from the free convection layer value to the value of θ at the base of the yet undisturbed stable profile. Interfacial

layers will vary in depth and character, however, to facilitate the analysis, they are represented by a step discontinuity, $\Delta\theta$, in the θ -profile at $z = h$, the nominal top of the convectively unstable boundary layer, where $\Delta\theta$ ranges from zero to a few centigrade degrees corresponding to the intensity of interfacial mixing. The level ζ is defined as the height at which the stable profile, extrapolated downwards, intersects the unstable profile and the term "overshoot" is used to denote the depth

$$\sigma = h - \zeta \qquad (1)$$

The extent of profile overshoot is clearly proportional to $\Delta\theta$ which in turn reflects the degree of physical overshoot and entrainment.

The unstable layer grows due to the effects of the external solar heating of the surface and the internal redistribution of heat arising from the entrainment of the capping stable air into the boundary layer (Ball, 1960), a possible subsidence arising from synoptic scale convergence being the only counter effect included. Figure 3 shows schematic θ -profiles separated by time δt and we note the change in the stable gradient due to the subsidence field.

Advection, radiation and evaporation are not considered although in certain circumstances each or all of these processes can be important. For example , advection processes rather than diurnal variation will mostly control the development of the boundary layer over the sea. Also, although it is probably safe to neglect radiation effects in relatively cloudless daytime conditions (Elliott, 1964), the study of moist cloud-topped mixed layers under a strong inversion (Lilly, 1968) requires radiative cooling from the cloud layer top as the principal mechanism for inducing convective mixing beneath the inversion

and entrainment across the interface.

The potential temperature profiles of Figure 3 are described by the equations,

$$\theta(z,t) = F(h-z)\,\theta_c(t) + F(z-h)\,\theta_s(z,t) \tag{2}$$

$$\theta_s(z,t) = \theta_o + \gamma(t)\,z \ , \tag{3}$$

where $\theta_c(t)$ is the potential temperature in the free-convection layer, $\theta_s(z,t)$, $z > h(t)$, is the potential temperature in the stable layer, θ_o is effectively the near surface temperature when $h(t) = 0$, $\gamma(t)$ is the gradient of θ in the stable layer, and $F(x)$ is the Heaviside function, generally defined by

$$F(x) = \begin{cases} 1 & x > 0 \\ 0 & x < 0 \ . \end{cases} \tag{4}$$

The heat balance equation in convective situations has been shown by the intensive theoretical treatments of Boussinesq type approximations by Ogura and Phillips (1962), Calder (1968) and Dutton and Fichtl (1969) to be simply,

$$\frac{\partial H}{\partial z} = -\rho c_p \frac{d\theta}{dt} = -\rho c_p \left[\frac{\partial \theta}{\partial t} + w(z)\frac{\partial \theta}{\partial z}\right] , \tag{5}$$

where $H(z,t)$ is the sensible eddy heat flux, $w(z)$ is the vertical velocity field, ρ is the mean air density in the boundary layer and c_p is the specific heat of air at constant pressure. We assume that there is no appreciable turbulent sensible heat flux in the stable layer,

$$H(z,t) = 0 \qquad z > h \ . \tag{6}$$

The derivatives of θ required in equation (5) follow from equation (2), where differentiation of the Heaviside function gives the Dirac δ-function,

$$\frac{\partial \theta}{\partial z} = \delta(h-z)(\theta_s - \theta_c) + F(z-h)\frac{\partial \theta_s}{\partial z} \tag{7}$$

$$\frac{\partial \theta}{\partial t} = \delta(h-z)(\theta_c - \theta_s)\frac{dh}{dt} + F(h-z)\frac{d\theta_c}{dt} + F(z-h)\frac{\partial \theta_s}{\partial t} \ . \tag{8}$$

With equations (6) - (8) equation (5) in the stable layer reduces to

$$\frac{\partial \theta_s}{\partial t} = -w(z)\frac{\partial \theta_s}{\partial z} \qquad z > h \ , \qquad (9)$$

which from (3) implies

$$\frac{1}{\gamma}\frac{d\gamma}{dt} = -\frac{w(z)}{z} = \beta \ , \qquad \text{say,}$$

i.e.

$$w(z) = -\beta z \qquad (10)$$

and

$$\gamma(t) = \gamma(0)\, e^{\beta t} \qquad (11)$$

where β, the convergence parameter, is more aptly termed the subsidence parameter since we consider only $w(z) \leq 0$. Thus the model implies a subsidence field linear with height which will increase the stability of the capping layer according to (11).

In the free convection layer equation (5) becomes

$$\frac{\partial H}{\partial z} = -\rho c_p \frac{d\theta_c}{dt} \qquad z < h \ , \qquad (12)$$

implying a sensible heat flux profile, linear in z,

$$H(z,t) = H(0,t) - \frac{z}{h}\left(H(0,t) - H(h,t)\right) \ , \qquad z < h \ , \qquad (13)$$

where as $z \longrightarrow h-$ we obtain for the sensible heat flux at the interface

$$H(h,t) = H(0,t) - \rho c_p h \frac{d\theta_c}{dt} \ . \qquad (14)$$

Finally, employing the technique used by Lilly (1968) we integrate (5) across the interface from $h-\epsilon$ to $h+\epsilon$ and take the limit as $\epsilon \to 0$ to obtain

$$H(h,t) = -\rho c_p \left(\frac{dh}{dt} - w(h)\right)\left(\theta_s(h,t) - \theta_c(t)\right) \qquad (15)$$

and if we write

$$\frac{dh}{dt} = w(h) + w_e(t) \ , \qquad (16)$$

then $w_e(t)$ is the rate at which stable air is entrained into the boundary layer and (15) reduces to

$$H(h,t) = -\rho c_p w_e(t)\, \Delta\theta \ ,$$

$$= -\rho c_p w_e(t)\, \gamma(t)\, \sigma(t) \ , \qquad (17)$$

from the geometry of the profiles in Figure 3. Equation (15) was

derived in a different, but equivalent, form by Ball (1960), and with the inclusion of a radiation flux by Lilly (1968). Equation (17) shows that if there is no overshoot then there is no contribution of heat into the boundary layer through mixing at the interface. However, when σ is zero the boundary layer can still develop since w_e may be non-zero.

The profile geometry gives

$$\gamma\zeta = \theta_c(t) - \theta_o \qquad (18)$$

which implies, from equation (1) and (14), that

$$\frac{d(\gamma h)}{dt} - \frac{d(\gamma\sigma)}{dt} = \frac{H(0,t) - H(h,t)}{\rho c_p h} \quad . \qquad (19)$$

Further, equations (10), (11) and (16) allow (17) to be rewritten

$$\frac{d(\gamma h)}{dt} = -\frac{H(h,t)}{\rho c_p \sigma} \quad . \qquad (20)$$

To obtain h(t) from equations (19) and (20) it is necessary to eliminate the overshoot $\sigma(t)$ which we have noted is closely related to the degree of mixing at the interface.

Consideration of the local turbulent kinetic energy balance allowed Ball (1960) and Lilly (1968) to formulate a relationship between H(h,t) and H(0,t). Lilly argues for the reduction of the full integrated turbulent kinetic energy equation to the form

$$-\int_0^h \frac{g}{\rho c_p \bar{\theta}} H(z,t)\, dz + T_h + \int_0^h \epsilon \, dz = 0 \qquad (21)$$

where the first term, in conventional notation, gives the integrated rate of production of energy due to buoyancy, T_h represents the pressure and energy transport terms at h and ϵ is the mean rate of molecular dissipation of turbulent kinetic energy. Then applying Ball's suggestion that the dissipation and transport terms can be neglected and inserting an eddy heat flux varying linearly with z (equation (13)) equation (21) yields Ball's hypothesis,

$$H(h,t) = -H(0,t) \qquad (22)$$

i.e. the heat gained by entrainment from above is equal to the heat supplied at the base. Ball's proposal that viscous dissipation is responsible for the destruction of a small part of the turbulent kinetic energy only is clearly open to question, particularly in the light of the experimental results of Deardorff, Willis and Lilly (1969) and the recently obtained profiles of ϵ throughout the boundary layer for different classes of stability (Rayment 1972 a, b) however the hypothesis does provide a maximum possible entrainment criterion and for the corresponding practical minimum entrainment criterion we adopt (Lilly, 1968)

$$H(h,t) = 0 \qquad (23)$$

To avoid questionable manipulation of the energy balance equation we shall assume that the heat brought into the boundary layer due to entrainment is a constant fraction of the surface sensible heat flux, thus

$$H(h,t) = -A\,H(0,t) \quad , \quad 0 \leq A \leq 1 \qquad (24)$$

This allows the possibility of any degree of interfacial mixing including the extreme cases, A = 1 (Ball's hypothesis) and A = 0 (minimum entrainment).

Dividing equation (19) by (20) and applying condition (24) we obtain

$$\frac{d(\gamma\sigma)}{d(\gamma h)} + \left(\frac{1+A}{A}\right)\frac{\sigma}{h} - 1 = 0 \qquad (25)$$

which, after integration, yields

$$\sigma = \alpha h \qquad (26)$$

where

$$\alpha = \frac{A}{1+2A} = \frac{H(h,t)}{2H(h,t) - H(0,t)} \qquad (27)$$

if $\sigma = 0$ when $h = 0$ and $\gamma \neq 0$. These solutions require the overshoot to be a constant fraction α of the depth of the evolving boundary layer where α is related to the degree of interfacial mixing through (27).

With σ replaced by αh equation (19) reduces to

$$\frac{d(\gamma h)}{dt} = \frac{H(0,t) - 2H(h,t)}{\rho c_p h} , \tag{28}$$

which can be expressed in a variety of forms,

$$\frac{dh^2}{dt} + 2\beta h^2 = \frac{2\left[H(0,t) - 2H(h,t)\right]}{\rho c_p \gamma(t)} \tag{29}$$

$$= \frac{2(1+2A)\,H(0,t)}{\rho c_p \gamma(t)} \tag{30}$$

$$= \frac{2H(0,t)}{(1-2\alpha)\rho c_p \gamma(t)} . \tag{31}$$

Integration of (29) gives

$$h^2(t) = h^2(t_o)e^{2\beta(t_o-t)} + 2e^{-2\beta t}\int_{t_o}^{t} e^{2\beta\tau}\frac{\left[H(0,\tau)-2H(h,\tau)\right]}{\rho c_p \gamma(\tau)}\,d\tau \tag{32}$$

for the evolution of the depth of the convectively unstable boundary layer which not only includes the effects of synoptic subsidence, a varying surface sensible heat flux, and the stability of the capping inversion but also the effects of any degree of interfacial mixing, determined by the ratio $H(h,t)/H(0,t)$.

The corresponding expression for the entrainment rate follows from equations (10), (11), (16) and (28)

$$w_e(t) = \frac{dh}{dt} - w(h) = \frac{1}{\gamma}\frac{d(\gamma h)}{dt} = \frac{H(0,t) - 2H(h,t)}{\rho c_p \gamma h} . \tag{33}$$

From (14), (24) and (32) we can write,

$$d\theta_c = \frac{(1+A)\,dI(t;t_o,\beta)}{\left[h^2(t_o)e^{2\beta t_o} + \frac{2(1+2A)}{\gamma(0)}I(t;t_o,\beta)\right]^{1/2}} , \tag{34}$$

where

$$I(t;t_o,\beta) = \int_{t_o}^{t}\frac{e^{\beta\tau}H(0,\tau)}{\rho c_p}\,d\tau , \tag{35}$$

and so the evolution of the profile is given by

$$\theta_c(t) = \theta_c(t_o) + \frac{(1+A)\gamma(0)}{(1+2A)}\left\{\left[h^2(t_o)e^{2\beta t_o} + \frac{2(1+2A)}{\gamma(0)}I(t;t_o,\beta)\right]^{1/2} - h(t_o)e^{\beta t_o}\right\} . \tag{36}$$

4. RESULTS FROM THE SIMPLE MODEL

There are several points of immediate interest.

(i) We note that heat entering the boundary layer from the top not only originates from interfacial mixing but contributes to further mixing and is therefore doubly effective in boundary layer growth.

(ii) Ball's hypothesis, A = 1 implying $\alpha = 1/3$, with $\beta = 0$ and h(0) = 0, gives

$$h^2(t) = 6 \int_0^t \frac{H(0,\tau)}{\rho c_p \gamma(0)} \, d\tau \, . \qquad (37)$$

The maximum growth rate is therefore $\sqrt{3}$ times the growth rate with no mixing across the interface. Equation (37) corrects Plate's (1971) expression for the case assuming Ball's hypothesis.

(iii) With $\beta = A = 0$ and a constant surface heat flux, H_o, equation (32) reduces to

$$h^2(t) = \frac{2 H_o t}{\rho c_p \gamma(0)} \, , \qquad (38)$$

the expression derived by Deardorff, Willis and Lilly (1969).

(iv) A simple sinusoidal heat flux is more realistic than constant surface heating when modelling the growth of the atmospheric convectively unstable boundary layer (Figure 1) and provides simple analytical expressions for h(t), $w_e(t)$ and $\theta_c(t)$.

Let

$$H(0,t) = \hat{H} \sin(\Omega t) \, , \qquad (39)$$

a good approximation close to an equinox, where Ω is the Earth's angular rotation and h(0) = 0, then integration of (30) gives

$$h^2(t) = \frac{2(1+2A)\, e^{-2\beta t}}{\rho c_p \gamma(0)} \, I(t;0,\beta) \, , \qquad (40)$$

where

$$I(t;0,\beta) = \frac{\hat{H}}{\rho c_p (\beta^2 + \Omega^2)} \left[e^{\beta t} (\beta \sin \Omega t - \Omega \cos \Omega t) + \Omega \right] . \qquad (41)$$

The effects of each parameter are best studied by considering the non-dimensional depth $h^*(t;\beta)$ where

$$h^{*2}(t;\beta) = \frac{h^2 \gamma(0) \Omega \rho c_p}{2(1+2A)\hat{H}}$$

$$= \frac{\Omega e^{-2\beta t}}{\beta^2+\Omega^2}\left[e^{\beta t}(\beta \sin \Omega t - \Omega \cos \Omega t) + \Omega\right]. \qquad (42)$$

Figure 4 illustrates h^* as a function of time for various values of β. In convective conditions β is typically about 0.6×10^{-5} sec^{-1} (Ball (1960), Lilly (1968)) implying a subsidence velocity of 0.6 cm sec^{-1} at a height of 1 km. Not only does the subsidence suppress the growth of the unstable layer but if sufficiently intense will eventually outweigh the entrainment rate and cause the boundary layer to decrease in depth even although heat may still be entering the boundary layer from below and possibly above. Figure 5 provides an alternative representation of h^* as a function of β and the non-dimensional heat flux $H^* = H(0,t)/\hat{H} = \sin \Omega t$.

The effects of different degrees of interfacial mixing, capping stability and surface sensible heat input are obtained by altering the $h^*(t;\beta)$ profile proportionally according to equation (42). Figure 6 shows the development of $h(t)$ for various degrees of interfacial mixing for typical values of $\gamma(0)$ and $\hat{H}$ in the cases of no subsidence and typical subsidence. The importance of interfacial mixing to the development of the layer is emphasized in the ultimate difference (1200m) between the extreme cases.

Figure 7 illustrates the non-dimensional entrainment rate

$$w_e^*(t;\beta) = \left[\frac{2\rho c_p \gamma(0)}{(1+2A)\Omega \hat{H}}\right]^{1/2} w_e = \frac{e^{-\beta t}\sin \Omega t}{h^*(t;\beta)}, \qquad (43)$$

which is a maximum at the start of the development ($\lim_{t\to 0} w_e^*(t;\beta) = \sqrt{2}$) and then decays steadily to zero.

The importance of the simple model is not so much that it is capable of giving the broad evolutionary features of the developing convectively unstable boundary layer but that it enables us to judge the relative importance of each of the contributing factors. In particular we note the importance to the development of heat flow into the boundary layer from above but to date we have no reliable estimate of the degree of interfacial mixing that can be achieved in the atmosphere. The answer to this problem must come from combined observational and theoretical study of interfacial mixing layers and the dynamics of the thermal convection which induces and maintains such processes.

In the meantime we shall consider the simple model in relation to the 1953 O'Neill data and the typical boundary layer development illustrated in Figure 1. We note immediately that the graph of $\langle h(t) \rangle$ does not have the simple shape suggested in Figure 6.

5. APPLICATION OF THE MODEL TO THE 1953 O'NEILL DATA

The development of the unstable boundary layer depends on the four parameters β , A, $\gamma(t)$, $H(0,t)$. In the following discussion the subsidence parameter will be neglected, bearing in mind, however, the suppressive role it can play. Also the mean O'Neill surface sensible heat flux, not being a simple sine wave, will be integrated graphically.

In the simple model $\gamma(0)$ and A have been assumed constant throughout any particular development. A study of actual temperature profiles shows that

$\partial\theta/\partial z$ varies with height and so strictly the gradient of potential temperature in the stable layer immediately above the mixed layer is a function not only of time but of the depth h(t). A detailed study of the O'Neill profiles suggests a minimum requirement of two distinct stages. In the early stages of the development the unstable layer is entraining the nocturnally established inversion which has a typical gradient of about 18×10^{-3} °K m^{-1} . We note from Figure 1 that these inversions are typically about 400m deep and will take between 2-4 hours to be eroded from below after which the unstable layer is capped by a stable, though not necessarily inverted layer, with gradient typically about 6×10^{-3} °K m^{-1} . The factor three between the stable θ-gradients which characterize each stage will obviously have marked effects on the nature of the development.

There remains our treatment of the parameter A which effectively measures the degree of interfacial mixing about which we have little direct knowledge. Strictly speaking our differential equation applies to any period when the ratio H(h,t)/H(0,t) is constant and the overshoot is a constant fraction of the depth of the boundary layer. Values of A at the O'Neill ascent times were inferred from equation (3) with $\beta = 0$ and h, dh/dt, H(0,t) and $\gamma(t)$ estimated from the profiles. Although there was a great deal of scatter the values obtained for A implied at least three stages in the development of the convectively unstable boundary layer. For the first half of the development A is close to zero, this is followed abruptly by a period of about four hours where A has a distinct non-zero value in the neighbourhood of $\frac{1}{2}$, and finally there follows a period with A again close to zero.

If we combine the stages suggested in Figure 1 and those suggested by the variations in time of γ and A we have five distinct Phases to represent the diurnal evolution of the land boundary layer in clear sky conditions with marked daytime insolation. In reality the development will proceed continuously through Phases 1-4, the strict discontinuities being between Phases 4 and 5 and Phases 5 and 1.

Phase 1. This begins about one hour after sunrise when the surface sensible heat flux becomes positive and begins to erode the nocturnally established surface inversion. Thermal penetration into the stable layer is quickly suppressed by the marked stable stratification. There is no significant interfacial mixing and the unstable boundary layer develops slowly through encroachment of the stable layer.

Phase 2. The nocturnal inversion has been eroded and the marked change in the stability of the capping layer and the strengthening of the thermals cause the development to proceed more rapidly. Interfacial mixing is still effectively slight but increasing.

Phase 3. The surface sensible heat flux is close to maximum value, thermal penetration of the stable layer is now at its peak and a true interfacial entrainment layer is established. Heat from above will be playing a significant role in the boundary layer's development.

Phase 4. The surface sensible heat flux remains positive but is decreasing and the weakening thermals are no longer able to maintain the thorough mixing throughout the established deep convection layer or their penetration of the stable layer. Interfacial mixing has decayed and subsidence, advection and

mechanical effects begin to dominate the evolution. The depth of the boundary layer remains steady or even begins to decrease.

Phase 5. About an hour or so before sunset the heat flux changes sign and the nocturnal inversion begins to develop. The boundary layer remains a shallow, slowly evolving, stable layer until about an hour after sunrise.

Phases 1-3 can be adequately described by equations (29)-(31) if we allow discontinuous changes in the values of A, and hence α and the entrainment rate, at the change over times between the phases. The depth during Phase i, i=1,2,3, defined by $t_{o,i} \leq t \leq t_{1,i}$, is given in the usual notation by

$$h^2(t) = h^2(t_{o,i})\, e^{2\beta(t_{o,i}-t)} + \frac{2(1+2A_i)\, e^{-2\beta t}}{\gamma_i(0)} \int_{t_{o,i}}^{t} e^{\beta\tau} \frac{H(0,\tau)}{\rho c_p}\, d\tau \,, \qquad (44)$$

where $h^2(t_{o,i}) = h^2(t_{1,i-1})$, and the entrainment rate by

$$w_e(t) = \frac{(1+2A_i)\, e^{-\beta t} H(0,t)}{\rho c_p \gamma_i(0)\, h(t)} \,, \qquad (45)$$

with a corresponding expression for $\theta_c(t)$.

With the multi-phase model an important application is forecasting the time of breakdown of the nocturnally established inversion. In the presence of subsidence the depth, η , of the inversion is given by

$$\eta(t) = \eta(0)\, e^{-\beta t} \,, \qquad (46)$$

t = 0 coinciding with $H(0,t) = h(t) = 0$, $\partial H(0,t)/\partial t > 0$, whereas the depth of the developing boundary layer is from (44),

$$h^2(t) = \frac{2(1+2A_1)}{\gamma_1(0)}\, e^{-2\beta t} \int_0^t e^{\beta\tau} \frac{H(0,\tau)}{\rho c_p}\, d\tau \,. \qquad (47)$$

At breakdown, $h(t) = \eta(t)$ and so from (46) and (47),

$$I(t_{1,1}; 0, \beta) = \int_0^{t_{1,1}} e^{\beta\tau} \frac{H(0,\tau)}{\rho c_p}\, d\tau = \frac{\gamma_1(0)\, \eta^2(0)}{2(1+2A_1)} \,. \qquad (48)$$

The time of breakdown is found by solving (48) for $t_{1,1}$.

With the simple sinusoidal heat flux model equation (48) can be expressed in terms of a non-dimensional inversion depth

$$\eta^*(0)[t_{1,1};\beta] = \eta(0)\left[\frac{\rho c_p \Omega \gamma_1(0)}{2(1+2A_1)\hat{H}}\right]^{1/2} = e^{\beta t_{1,1}} h^*(t_{1,1};\beta) \qquad (49)$$

which must be solved for $t_{1,1}$. Figure 8 shows $\eta^*(0)$ as a function of $t_{1,1}$ and β and with $\beta = A_1 = 0$, $\eta(0) = 400$ m, $\gamma_1(0) = 18 \times 10^{-3}$ °K m^{-1} and a maximum heat flux of 30 mwatt cm^{-2}, $t_{1,1}$ is about 3 hours in good agreement with observations at O'Neill.

Figure 9 illustrates the rate of entrainment in a simple two-phase model with first phase as described above and $\gamma_2(0) = 6 \times 10^{-3}$ °K m^{-1} in the second phase. The first phase, lasting 3 hours, has no interfacial mixing and the subsequent development in the second phase is given for several values of A_2. We note the rapid acceleration in the entrainment rate immediately after breakdown of the nocturnal inversion even when $A_2=0$ and the change is due entirely to the change from γ_1 to γ_2.

Figure 10 compares the mean observed depth of the O'Neill boundary layer with several theoretical evolutions based on a three-phase model assuming $\beta = 0$ and the mean O'Neill heat flux. Values adopted for the governing parameters are $\gamma_1(0) = 18 \times 10^{-3}$ °K m^{-1}, $\gamma_2(0) = \gamma_3(0) = 6 \times 10^{-3}$ °K m^{-1}, $h(t_{1,1}) = \eta(t_{1,1}) = \eta(0) = 400$m, $h(t_{1,2}) = 850$m, $A_1 = A_2 = 0$ and A_3 takes several values in the range 0 to 1. Interfacial mixing has been delayed until the third phase and we see here the evidence for suggesting $A_3 = \frac{1}{2}$. Phase 4 requires a model which can account for the decay of the convective mixing within the boundary layer. With $A_3 = \frac{1}{2}$ the correlation coefficient between the predicted and observed mean depths is almost 1 and the standard error of estimation of the mean depth is about 70m (the observed depths however are in themselves accurate only to

within about 100m).

Figure 11 represents the evolution of h(t) as a function of $H(0,t)$ for the adopted three-phase model allowing for heat flux curves of different amplitude but similar shape to the mean O'Neill curve. Contours are drawn for different values of $\hat{H}$, the maximum surface sensible heat flux, and also for the time taken to evolve to a given stage.

When applied to individual O'Neill cases the mean model produced a correlation coefficient between predicted mean depths and observed actual depths, $h_o(t)$, of 0.86 with a standard error of estimation about the 45^o line of 345m.

The actual heat flux estimates at O'Neill could be in error by as much as 50% and so it was not desirable to replace the mean heat flux values by actual values. However, in Figure 12 we note the importance of choosing $\gamma(t)$ appropriate to the occasion. With $\gamma(t)$ estimated from individual profiles the three-phase model produces the correlation between observed and predicted depths of the convectively unstable boundary layer shown in Figure 13. The correlation coefficient is 0.93 and the standard error of estimation about the line $h_o(t) = h(t)$ is 255m. Period 5 produced the worst fit and indeed was the most difficult period for estimating h_o due to marked advection effects (Hanna (1969), Carson (1971)). The rogue point in Period 2 implies that we have arrived at Phase 3 about an hour too soon. Bearing in mind the errors in estimating $h_o(t)$ (Hanna (1969), Carson (1971)), the results from applying the modified simple model to actual data are very encouraging.

6. CONCLUSIONS

A model is proposed which describes the evolution of the convectively unstable boundary layer accounting for the effects of a diurnal pattern in the

surface sensible heat flux, a subsiding, capping stable layer and entrainment of the stable air into the boundary layer due to interfacial mixing which results in a heat flow into the boundary layer at its top. Equation (29) allows us to assess the relative importance of each of the contributing factors in the boundary layer's development and, in particular, we have noted the twofold effect of interfacial mixing.

No attempt has been made to model the dynamics of the important interfacial mixing but modification of the simple model based on the 1953 O'Neill data leads to a multi-phase model which prompts the provisional proposal that interfacial mixing is most important for a period in the early afternoon following the time of maximum surface heating. During this period at O'Neill we estimate $\frac{1}{2}$ for the ratio of the heat flux entering the boundary layer at the top to that entering at the surface. There is no evidence in the O'Neill data to support Ball's hypothesis that the ratio is near unity, indeed for a large part of the development the suggestion is that the interfacial mixing contribution is effectively zero, particularly in the early stages when the capping layer is the markedly stable, nocturnally established inversion. These deductions, being model dependent, are naturally speculative and we must look to the future development of studies such as those by Readings, Golton and Browning (1972) and Browning, Starr and Whyman (1972) for our answers. The part played by wind shear in the ultimate breakdown of the convoluted interface is a primary concern.

The multi-phase model is capable of producing realistic boundary layer development (Figures 10 and 13) and such representations in various conditions would be of great practical importance in schemes for estimating the vertical dispersion of pollutants. A provisional attempt to include such non-steady

boundary layer features in a practical scheme has already been outlined by Smith (1972).

The model should strictly be limited to the dry, convectively unstable boundary layer in virtually clear-sky, non-advective conditions. Important extensions to non-steady, fog layers or moist cloud-topped mixed layers will require extensive treatment of complex radiative and evaporative processes (see for example Lilly (1968)).

ACKNOWLEDGMENTS

The author wishes to thank Drs F B Smith and F Pasquill for their sustained interest in this work. Dr Smith in particular has provided many helpful and critical discussions.

REFERENCES

Ball, F K — 1960 — 'Control of inversion height by surface heating', Quart J R Met Soc., 86, pp. 483-494

1962 — Discussion on Ball's 1960 paper, Ibid., 88, pp. 102-105.

Browning K A, Starr J R and Whyman A J. — 1972 — 'The structure of an inversion above a convective boundary layer as observed using a high-power pulsed Doppler Radar', Paper presented at I.U.C.R.M. Conference, San Diego, June 1972.

Calder K L — 1968 — 'In clarification of the equations of shallow-layer thermal convection for a compressible fluid based on the Boussinesq approximation', Quart. J R Met. Soc., 94, pp. 88-92.

Carson D J — 1971 — 'On the thickness of the planetary boundary layer in diabatic conditions', Unpublished Meteorological Office Report, Turbulence and Diffusion Notes No 18.

Charnock H — 1972 — 'Air-sea interaction and the boundary layer' Contribution to Discussion Meeting, November 1971, on 'The global atmospheric research programme GARP and the United Kingdom's participation' Quart. J R Met. Soc., 98, pp. 447-459.

Charnock H and Ellison T H — 1967 — 'The boundary layer in relation to large-scale motions of the atmosphere and ocean' Study Conference on GARP (ICSU/IUGG, WMO and COSPAR), Stockholm 1967, Appendix III, pp 1-16.

Clarke R H — 1970a — 'Observational studies in the atmospheric boundary layer' Quart. J R Met. Soc., 96, pp. 91-114

1970b — 'Recommended methods for the treatment of the boundary layer in numerical models' Australian Met. Mag., 18, pp 51-73.

Deardorff J W — 1972a — 'Parameterization of the planetary boundary layer for use in general circulation models' Mon. Weath. Rev., 100, pp 93-106.

Deardorff J W 1972b 'Rate of growth of the nocturnal boundary layer', Proceedings of the Symposium on Air Pollution, Turbulence and Diffusion, December 1971, New Mexico, Ed. H W Church and R E Luna, pp. 183-190.

Deardorff J W and Willis G E 1967 'The free-convection temperature profile', Quart. J R Met. Soc., 93, pp 166-175.

Deardorff J W, Willis G E and Lilly D K 1969 'Laboratory investigation of non-steady penetrative convection', J Fluid Mech., 35, pp 7-31.

Delsol F, Miyakoda K and Clarke R H 1971 'Parameterized processes in the surface boundary layer of an atmospheric circulation model', Quart J R Met. Soc., 97 pp 181-208.

Dutton J A and Fichtl G H 1969 'Approximate equations of motion for gases and liquids', J Atmos. Sci., 26, pp 241-254.

Elliott W P 1964 'The height variation of vertical heat flux near the ground', Quart J R Met. Soc., 90, pp 260-265.

Hanna S R 1969 'The thickness of the planetary boundary layer', Atmos. Envir., 3 , pp 519-536.

Lettau H H and Davidson B 1957 'Exploring the Atmosphere's First Mile', Pergamon Press, London, New-York and Paris, 2 vols.

Lilly D K 1968 'Models of cloud-topped mixed layers under a strong inversion', Quart J R Met. Soc., 94 pp 292-309.

Ogura Y and Phillips N A 1962 'Scale analysis of deep and shallow convection in the atmosphere', J Atmos. Sci., 19, pp 173-179.

Plate E J 1971 'Aerodynamic Characteristics of Atmospheric Boundary Layers', USAEC Division of Technical Information Extension, Oak Ridge, Tennessee.

Rayment R 1972a Discussion on Clarke's 1970 paper, Quart J R Met. Soc., 98, pp 231-235.

1972b 'An observational study of the vertical profile of the high-frequency fluctuations of the wind in the atmospheric boundary layer', Unpublished Meteorological Office Report, Turbulence and Diffusion Notes No 22.

Readings C J, Golton E and Browning K A.	1972	'Fine-scale structure and mixing within an inversion'. Paper presented at I.U.C.R.M. Conference, San Diego, June 1972. Also available as Unpublished Meteorological Office Report, Turbulence and Diffusion Notes No 24.
Smith F B	1968	'A review of some recent theories of the boundary layer of the atmosphere'. Met Office, Met. Res. Cttee., MRCP 233 (Unpublished).
	1972	'A scheme for estimating the vertical dispersion of a plume from a source near ground-level'. First draft, extended summary. Unpublished Meteorological Office Report.
Townsend A A	1962	'Natural convection in the earth's boundary layer'. Quart J R Met. Soc., 88, pp 51-56.
Webb E K	1958	'Vanishing potential temperature gradients in strong convection'. Ibid., 84, pp 118-125.

FIGURE LEGENDS

Figure 1. The mean boundary layer thickness, $\langle h(t) \rangle$, and the sensible heat flux at the surface, $\langle H(0,t) \rangle$, deduced for the O'Neill data and plotted with standard errors as functions of time of day, t, in Mean Solar Time.

Figure 2. Schematic representation of the developing convectively unstable boundary layer and the adopted potential temperature profile, $\theta(z)$.

Figure 3. Adopted potential temperature profiles as a function of z and t and a representation of the parameters $h, \zeta, \Delta\theta, \gamma, \theta_o$ and θ_c.

Figure 4. The non-dimensional depth h^* as a function of time and various values of the subsidence parameter β. Sinusoidal heat flux model.

Figure 5. The non-dimensional depth h^* as a function of the subsidence parameter β and the non-dimensional sinusoidal heat flux H^*.

Figure 6. The development of the depth of the convectively unstable boundary layer, h(t), for various degrees of interfacial mixing, for typical values of $\gamma(0)$ and $\hat{H}$ in the cases of no subsidence and typical subsidence. Sinusoidal heat flux model.

Figure 7. The non-dimensional entrainment rate w_e^* as a function of time for various values of the subsidence parameter β. Sinusoidal heat flux model.

Figure 8. The non-dimensional height, $\eta^*(0)$, of the top of the nocturnally established surface inversion layer as a function of the inversion breakdown time, $t_{1,1}$, and subsidence parameter β. Sinusoidal heat flux model.

Figure 9. The entrainment rate $w_e(t)$ for a two-phase model characterized by the given parameters. Sinusoidal heat flux model.

Figure 10. Comparison of the mean observed depth of the O'Neill boundary layer with several theoretical evolutions based on a three-phase model and the mean O'Neill heat flux.

Figure 11. A three-phase model representation of h(t) as a function of H(0,t), assuming heat flux curves of different amplitudes but similar shape to the mean O'Neill curve. The broken contour lines give the time in hours to evolve to a particular stage.

Figure 12. The dependence of the evolution of h(t), in a typical three-phase model, on the choice of γ_2 and γ_3.

Figure 13. The depth of the O'Neill boundary layer, $h_o(t)$, estimated from profiles, against the depth, h(t), predicted using a three-phase model. The broken lines are $h_o(t) = h(t) \pm 255$m, where 255m is the standard error about the line $h_o(t) = h(t)$, the correlation coefficient being 0.93.

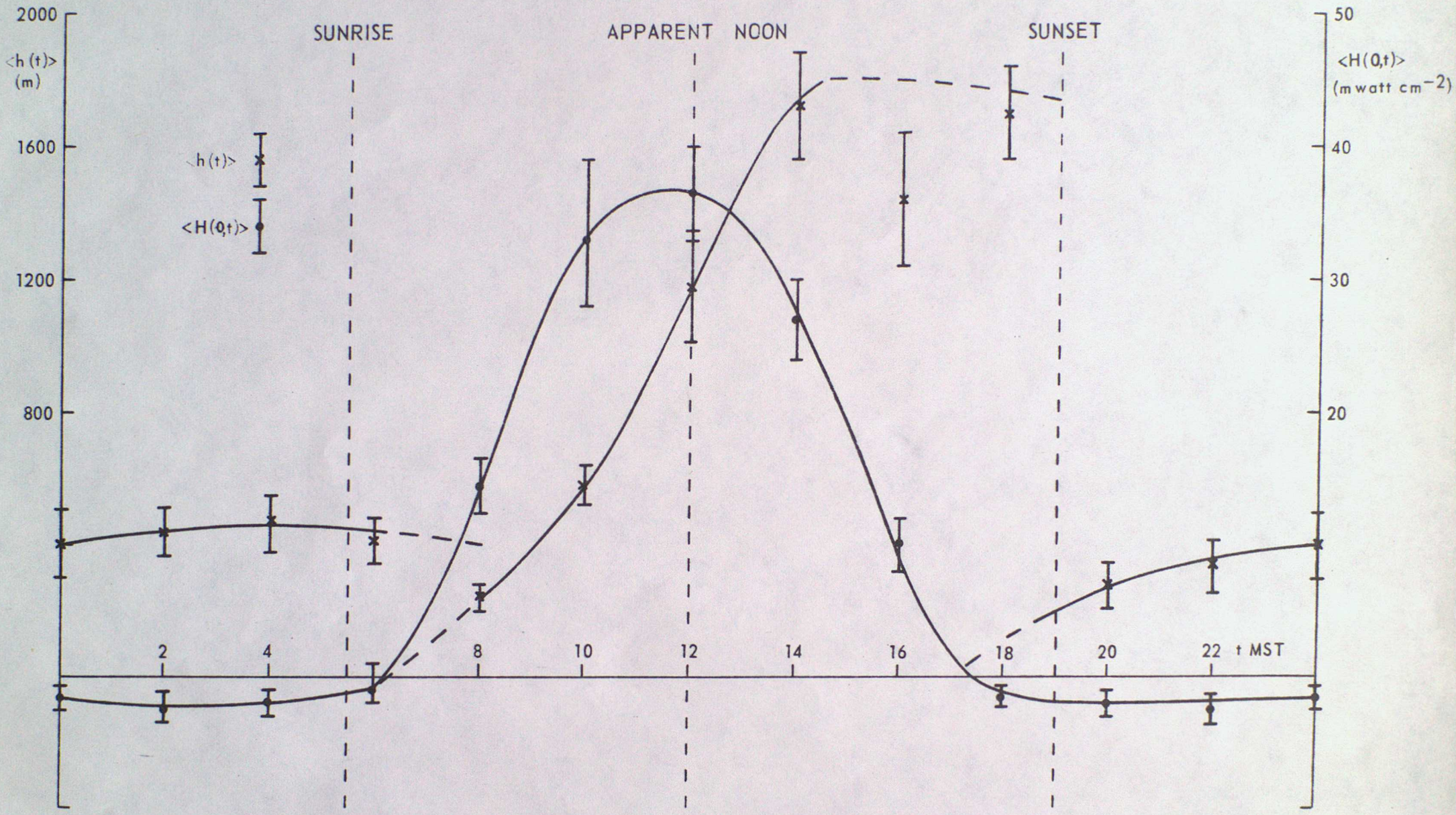

Figure 1. The mean boundary layer thickness, $\langle h(t) \rangle$ and sensible heat flux at the surface, $\langle H(0,t) \rangle$, deduced for the O'Neill data and plotted with standard errors as functions of time of day, t, in Mean Solar Time.

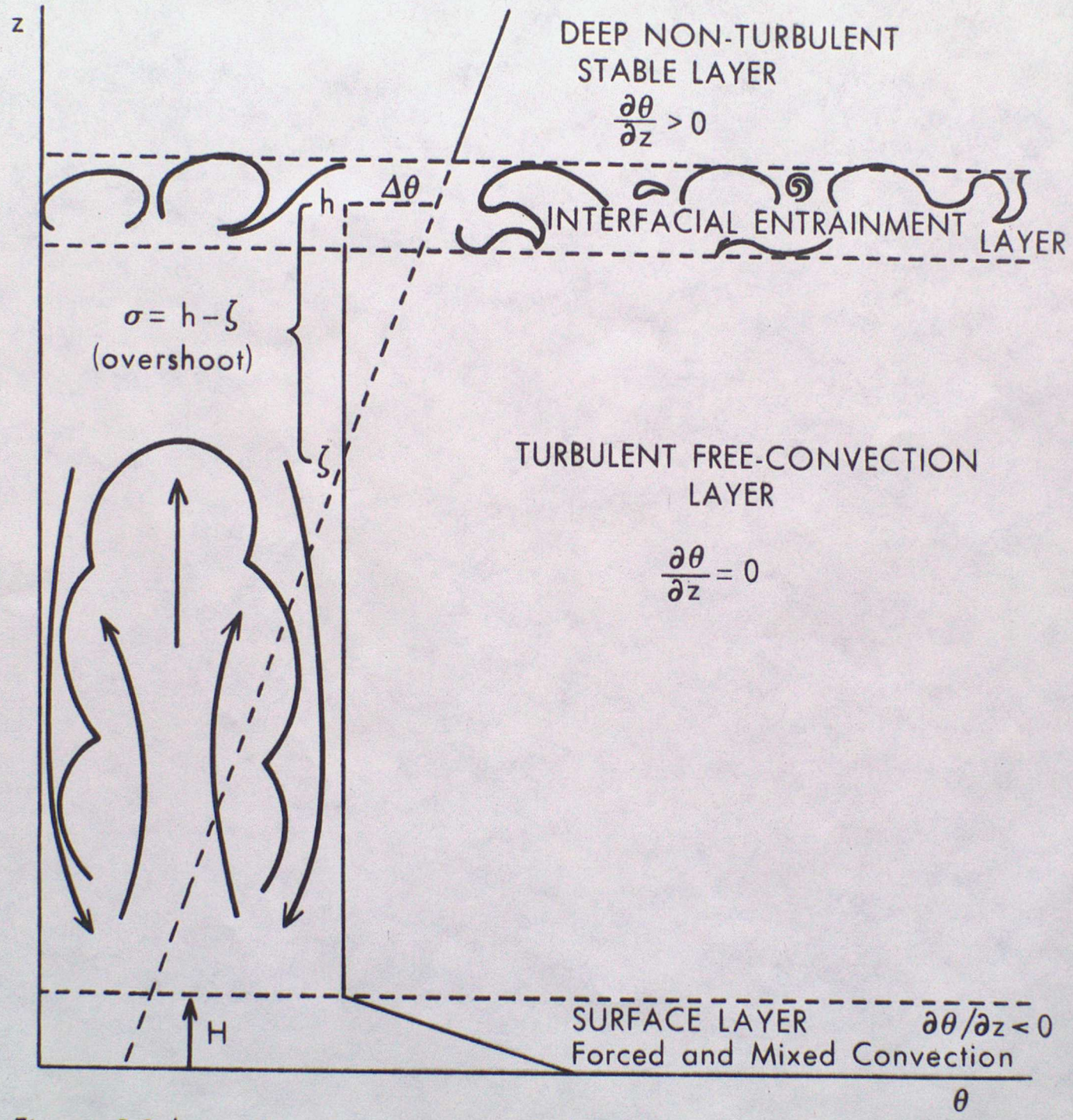

Figure 2.Schematic representation of the developing convectively unstable boundary layer and the adopted potential temperature profile, $\theta(z)$.

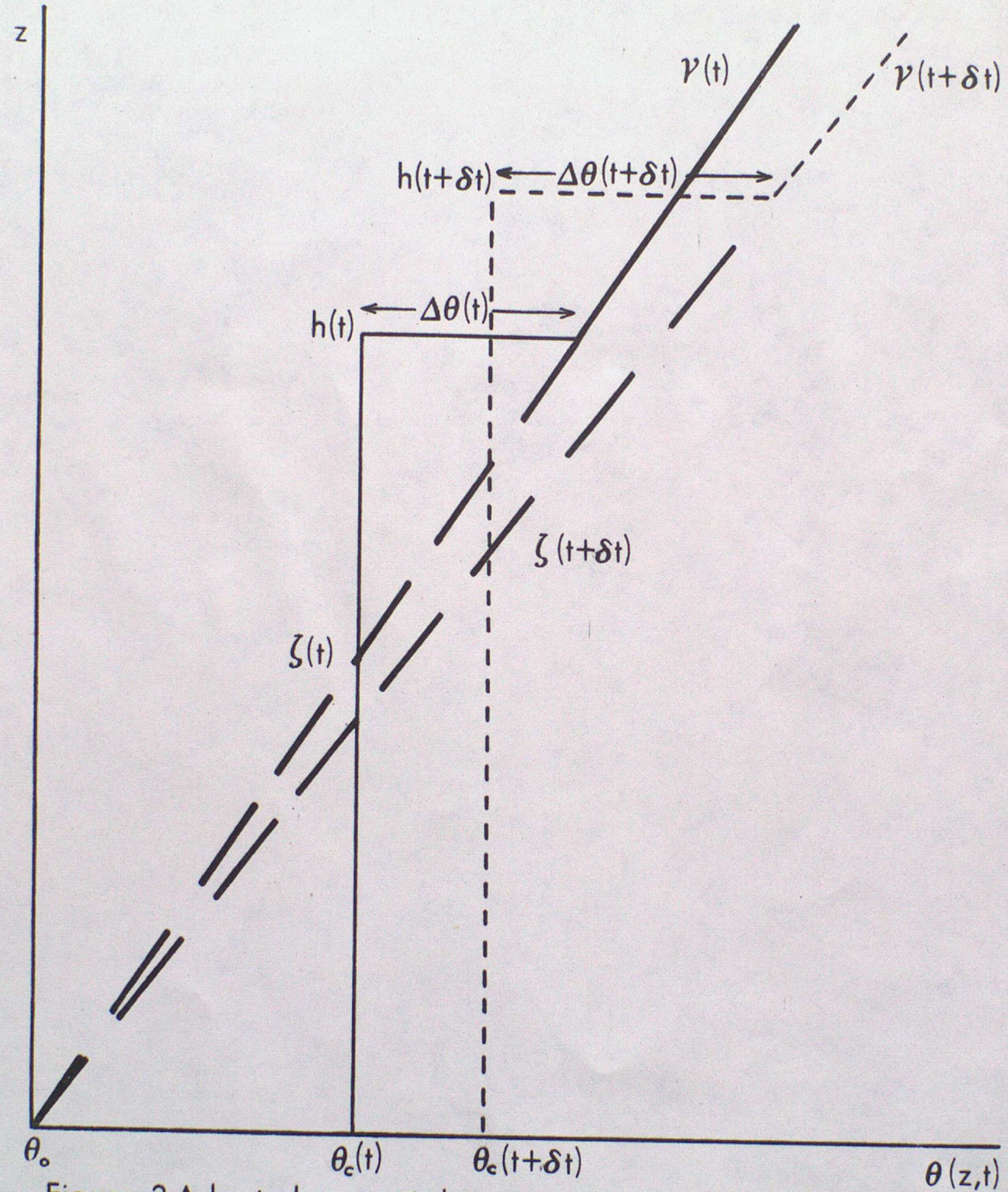

Figure 3. Adopted potential temperature profiles as a function of z and t and a representation of the parameters h, ζ, $\Delta\theta$, γ, θ_0 and θ_c.

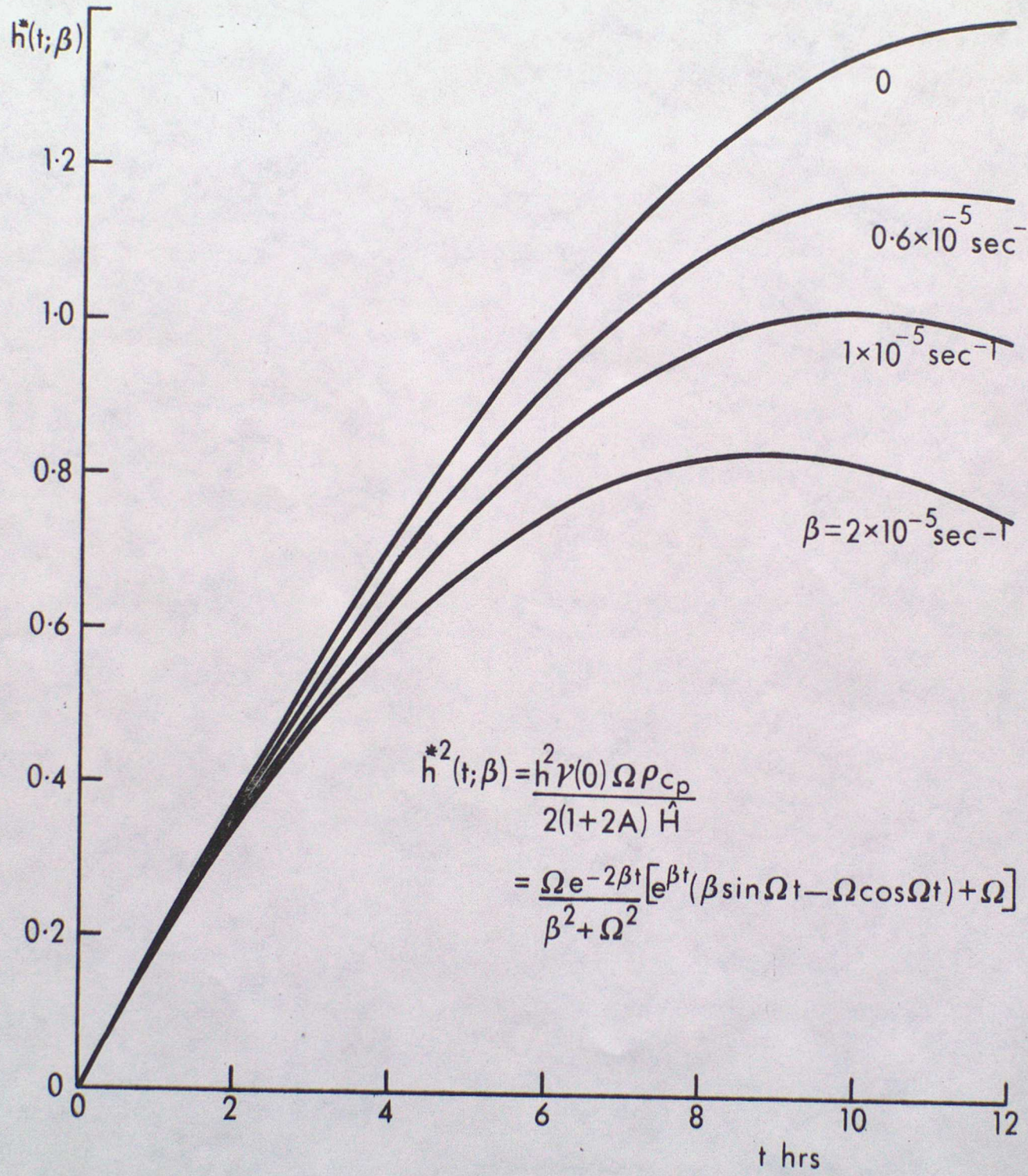

Figure 4. The non-dimensional depth h^* as a function of time and various values of the subsidence parameter β. Sinusoidal heat flux model.

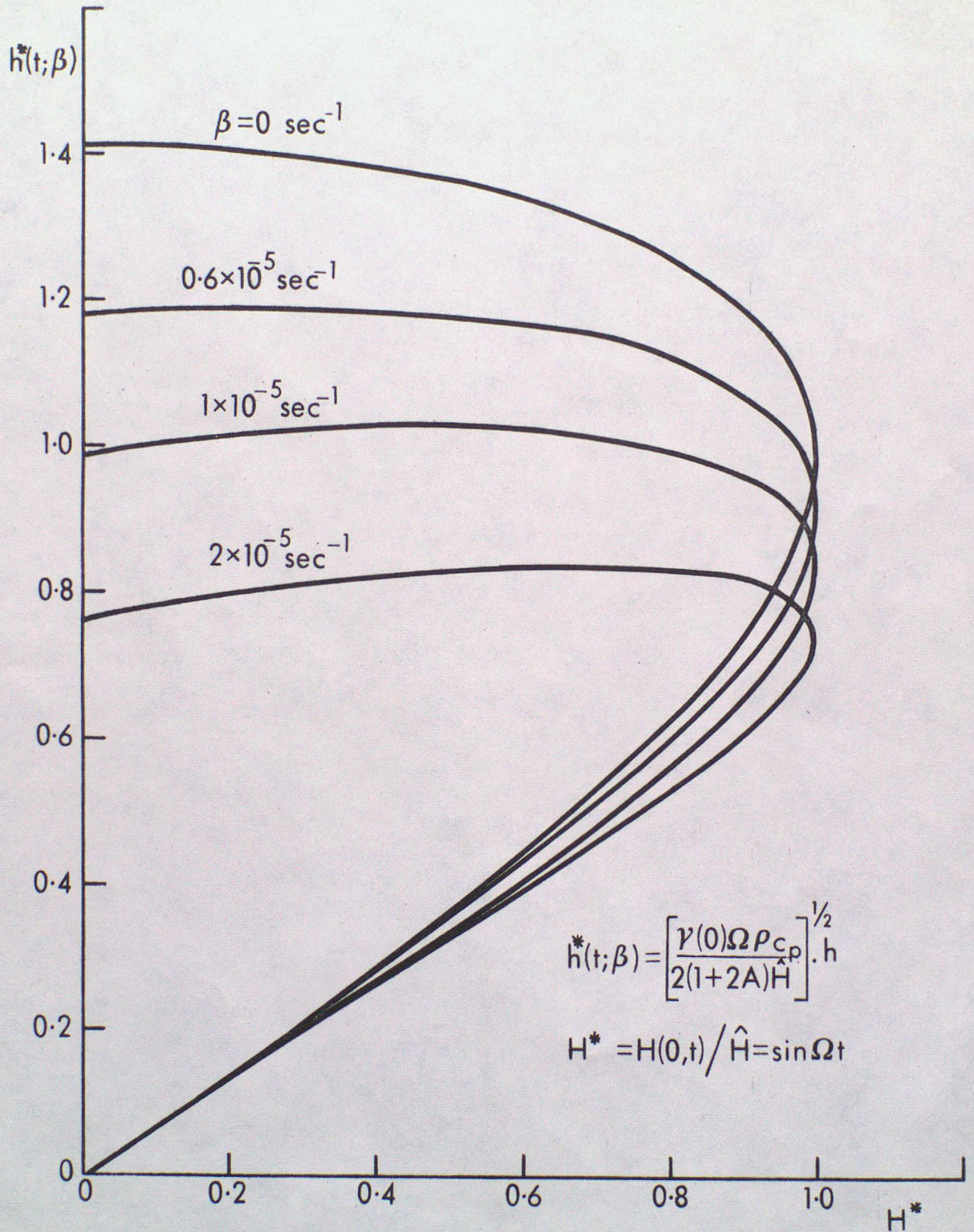

Figure 5.The non-dimensional depth h^* as a function of the subsidence parameter β and the non-dimensional sinusoidal heat flux H^*

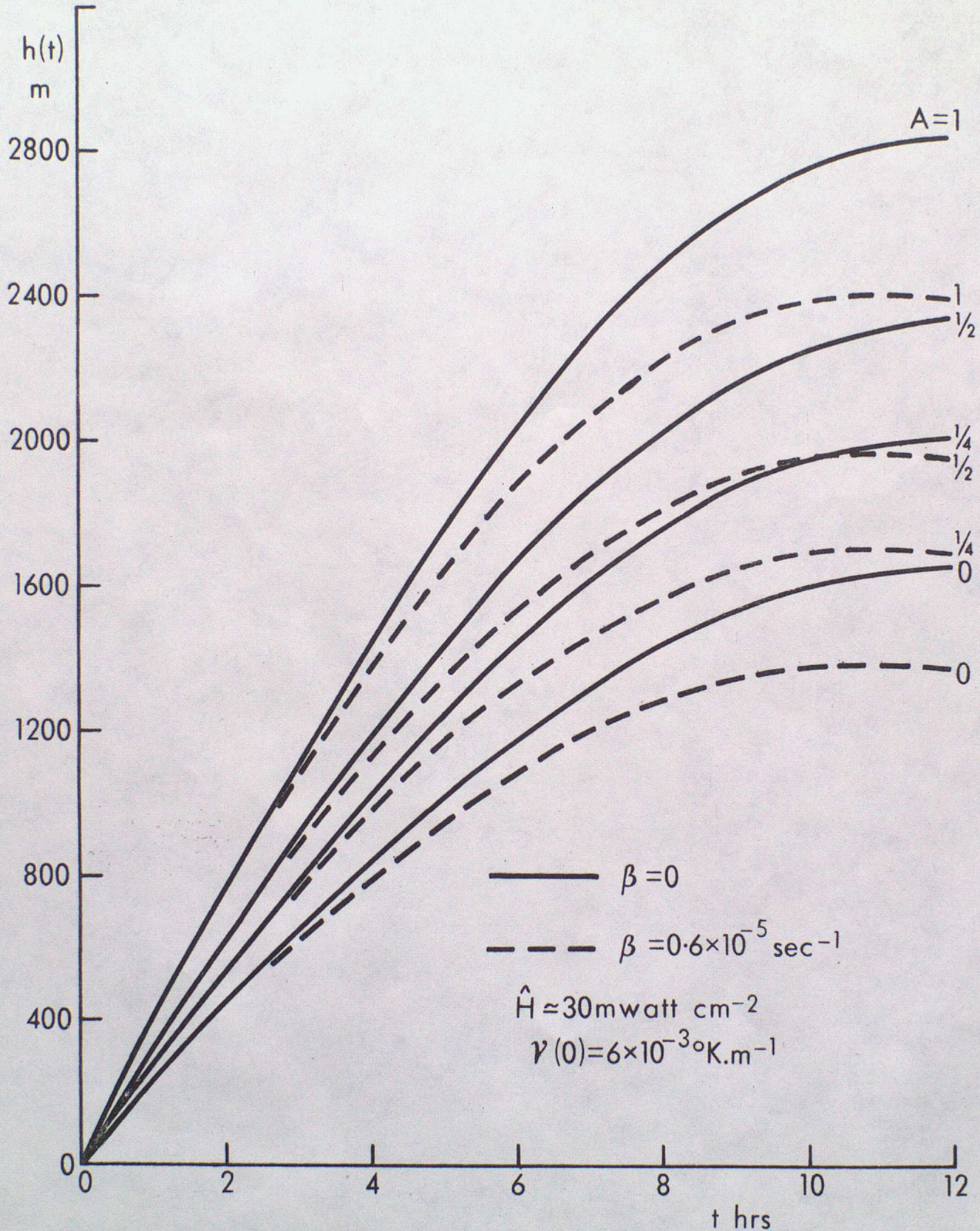

Figure 6. The development of the depth of the convectively unstable boundary layer, h(t), for various degrees of interfacial mixing, for typical values of $\gamma(0)$ and $\hat{H}$ in the cases of no subsidence and typical subsidence. Sinusoidal heat flux model.

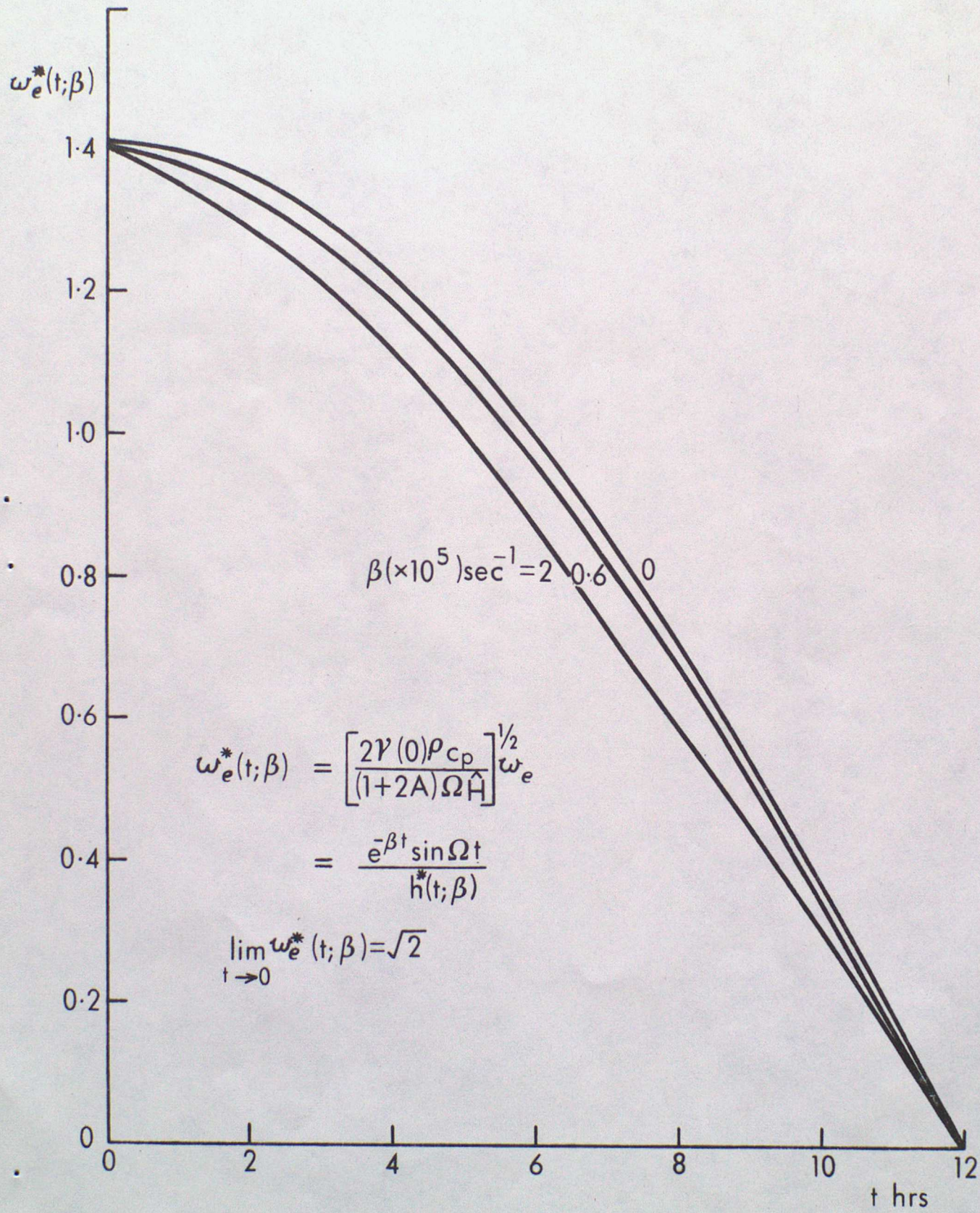

Figure 7. The non-dimensional entrainment rate ω_e as a function of time for various values of the subsidence parameter β Sinusoidal heat flux model.

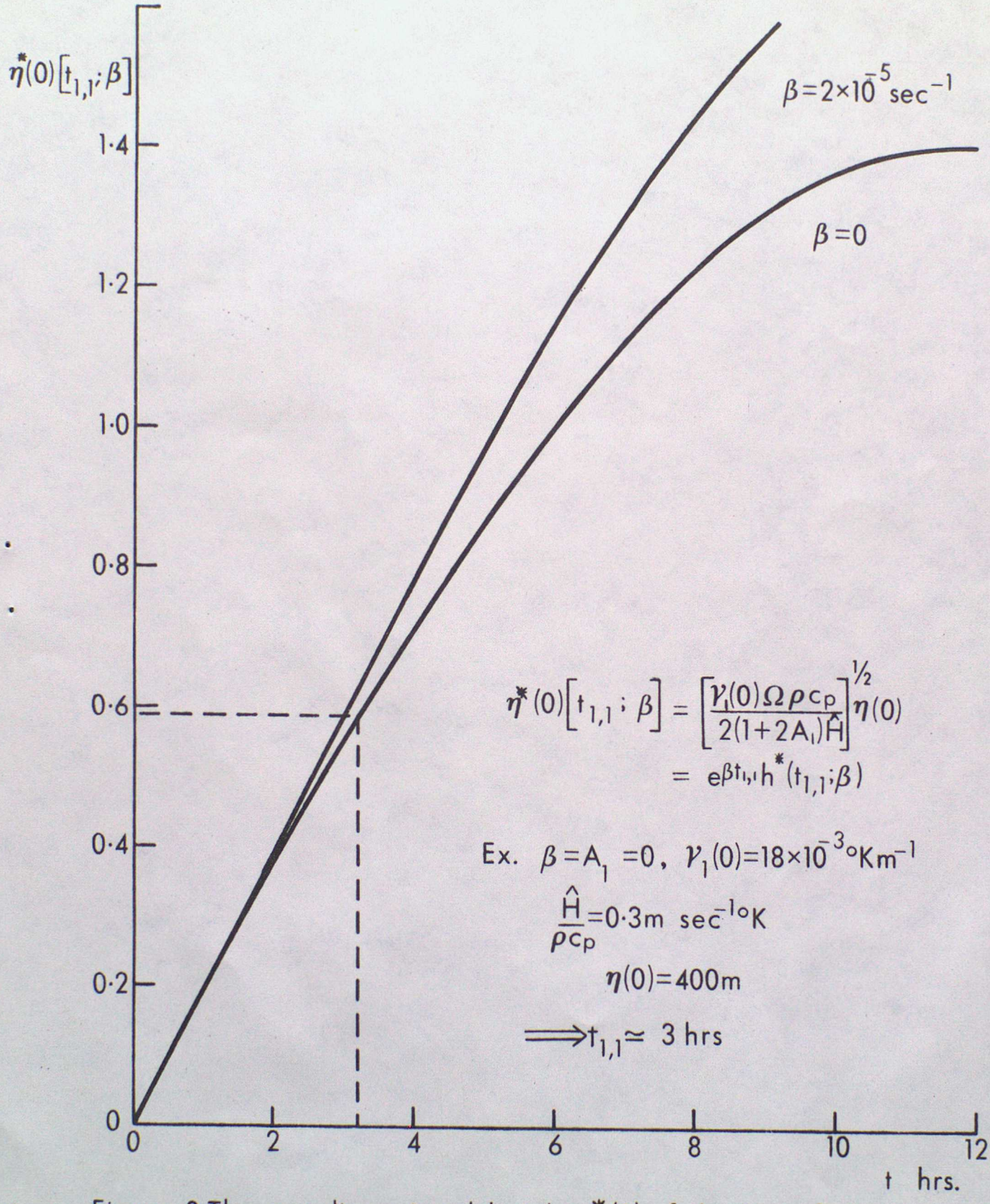

Figure 8. The non-dimensional height, $\eta^*(0)$, of the top of the nocturnally established surface inversion layer as a function of the inversion breakdown time, $t_{1,1}$, and subsidence parameter β.
Sinusoidal heat flux model.

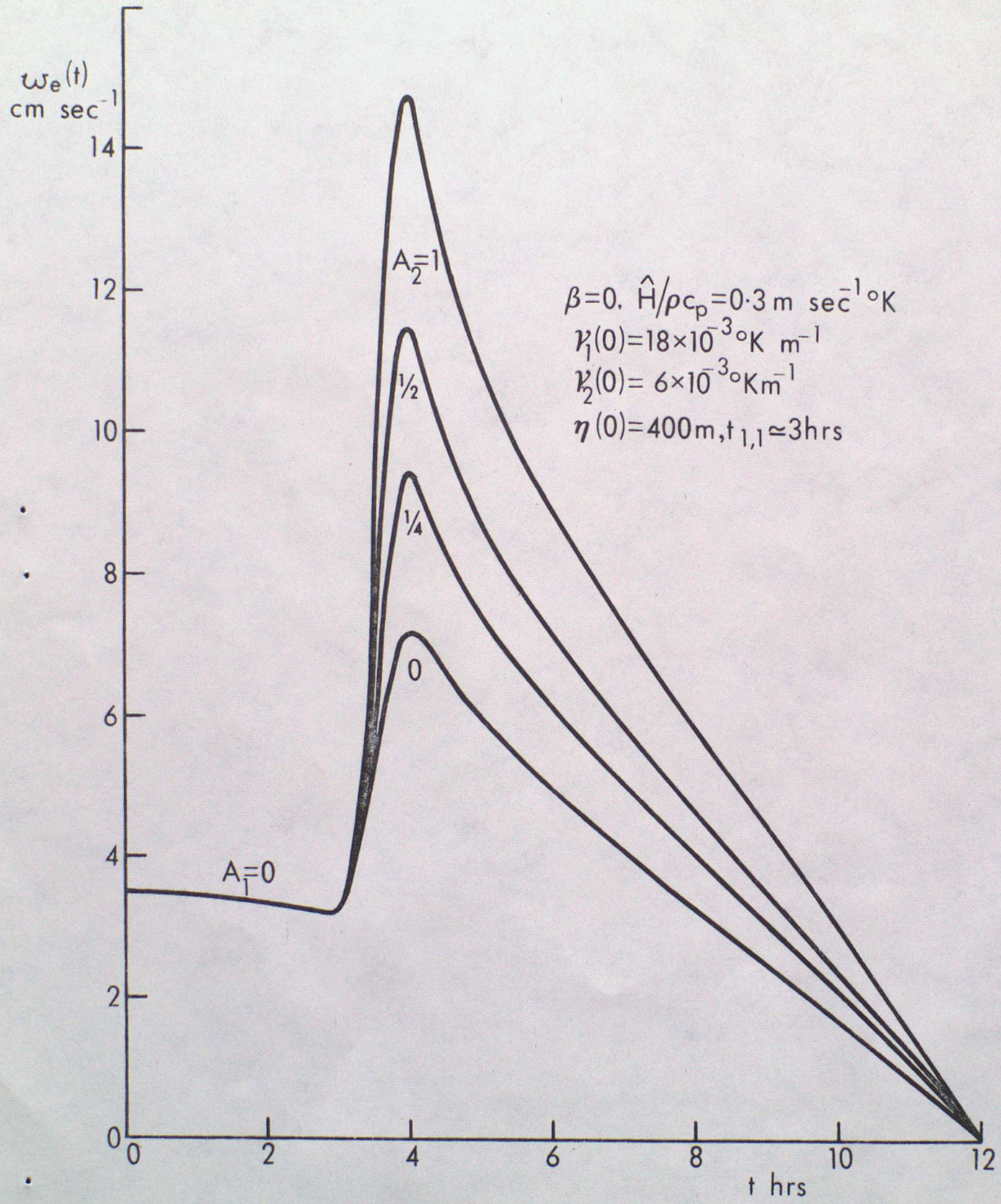

Figure 9. The entrainment rate $\omega_e(t)$ for a two-phase model characterised by the given parameters. Sinusoidal heat flux model.

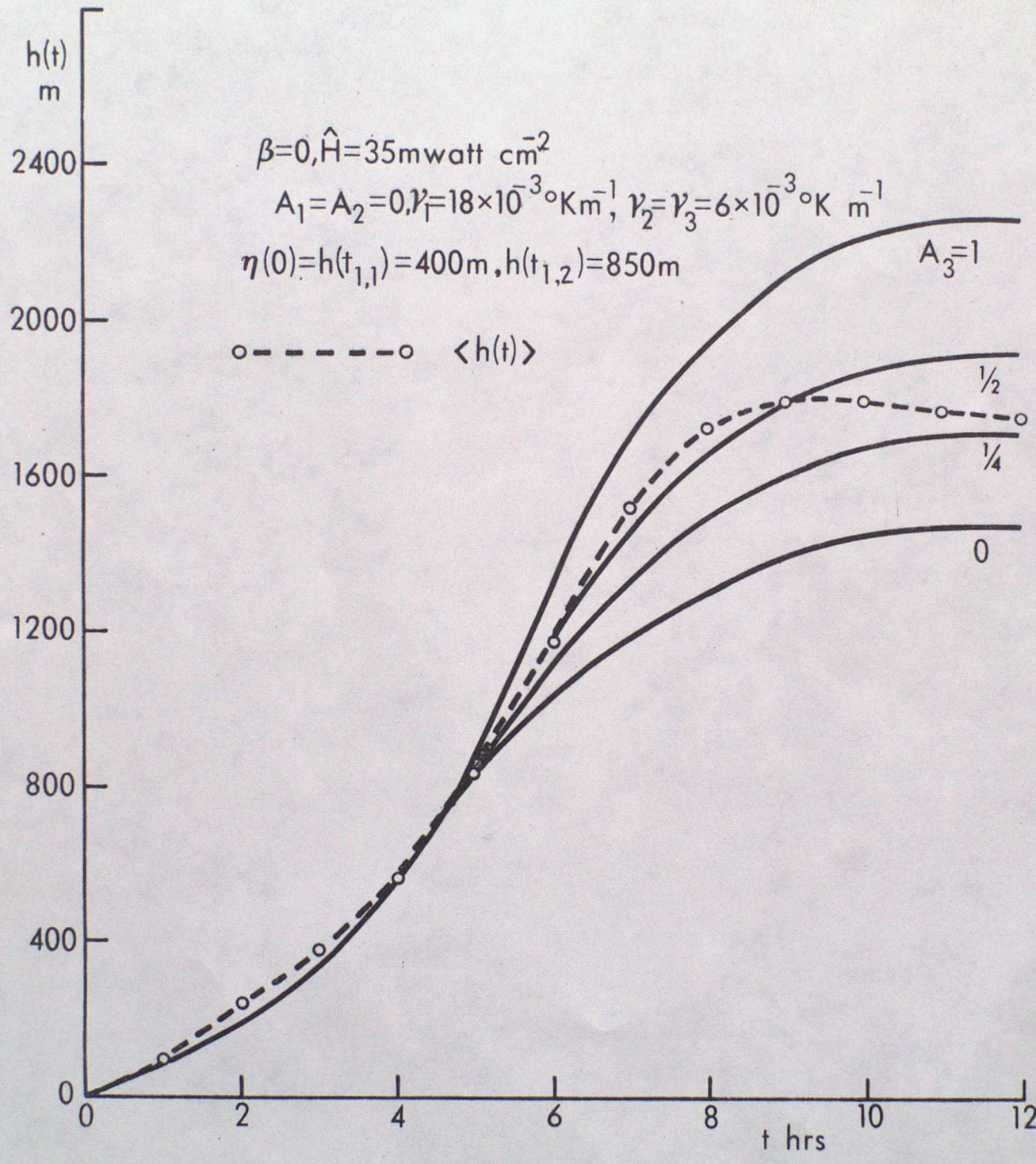

Figure 10. Comparison of the mean observed depth of the O'Neill boundary layer with several theoretical evolutions based on a three-phase model and the mean O'Neill heat flux.

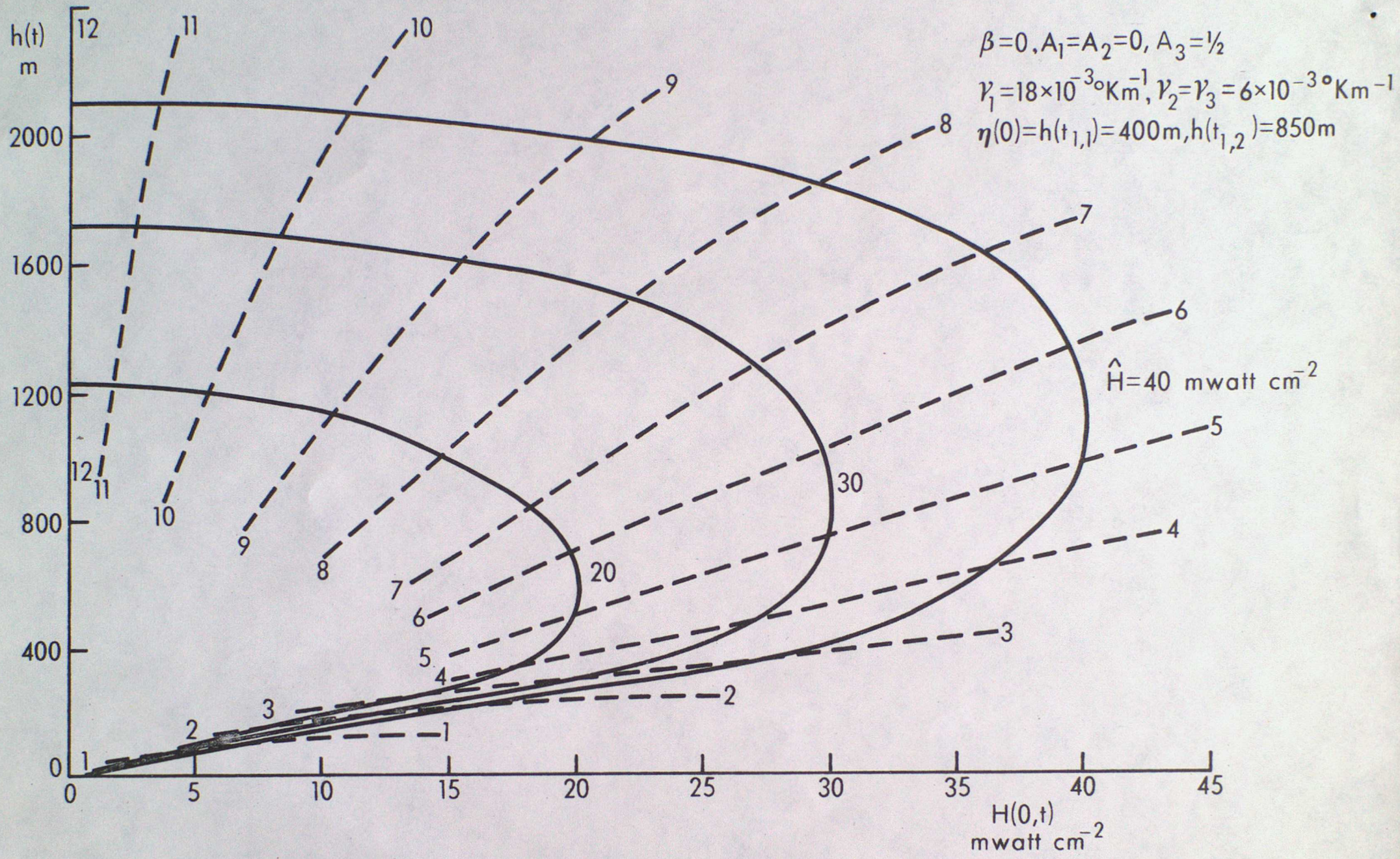

Figure 11. A three-phase model representation of h(t) as a function of H(0,t), assuming heat flux curves of different amplitudes but similar shape to the mean O'Neill curve. The broken contour lines give the time in hours to evolve to a particular stage.

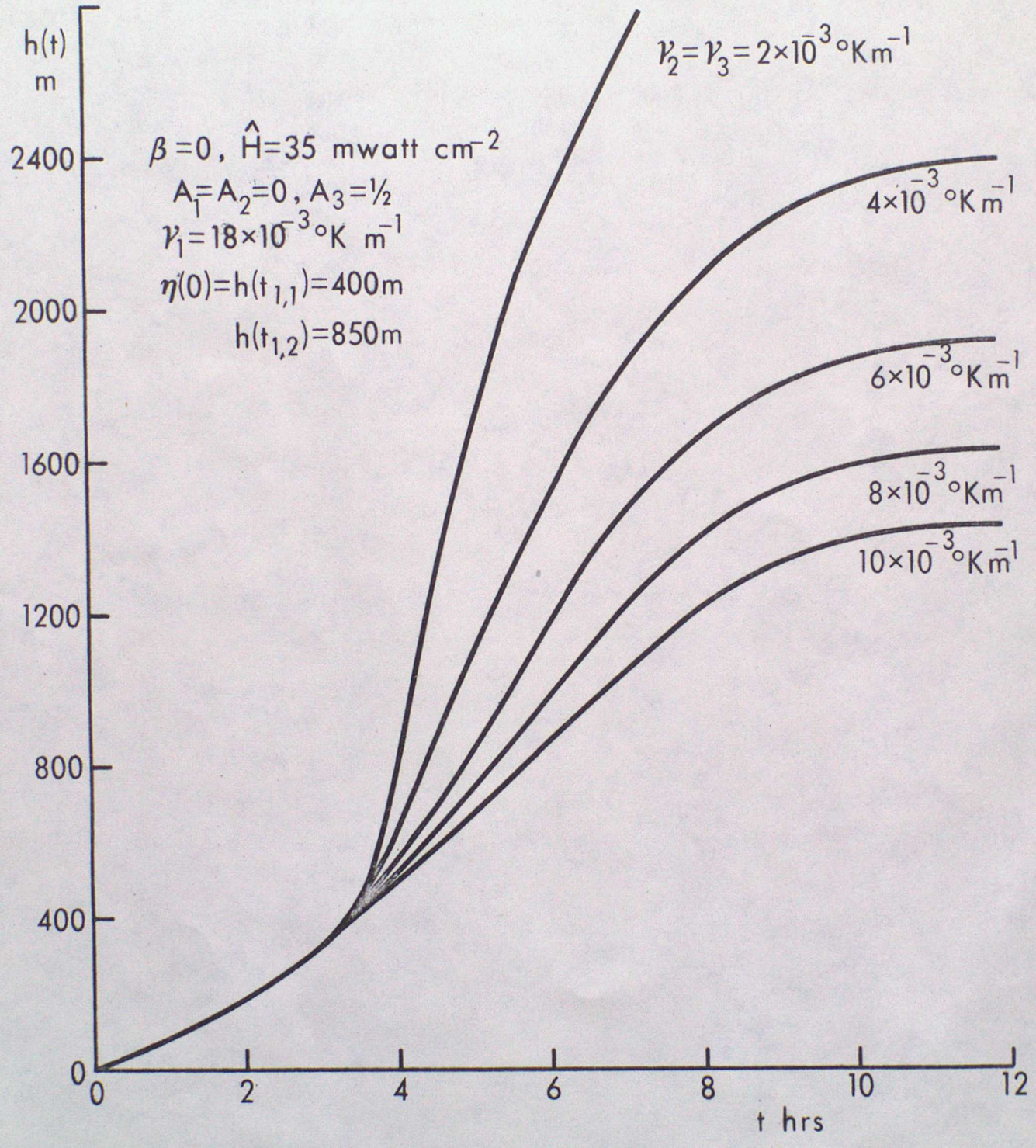

Figure 12. The dependence of the evolution of h(t), in a typical three-phase model, on the choice of ν_2 and ν_3.

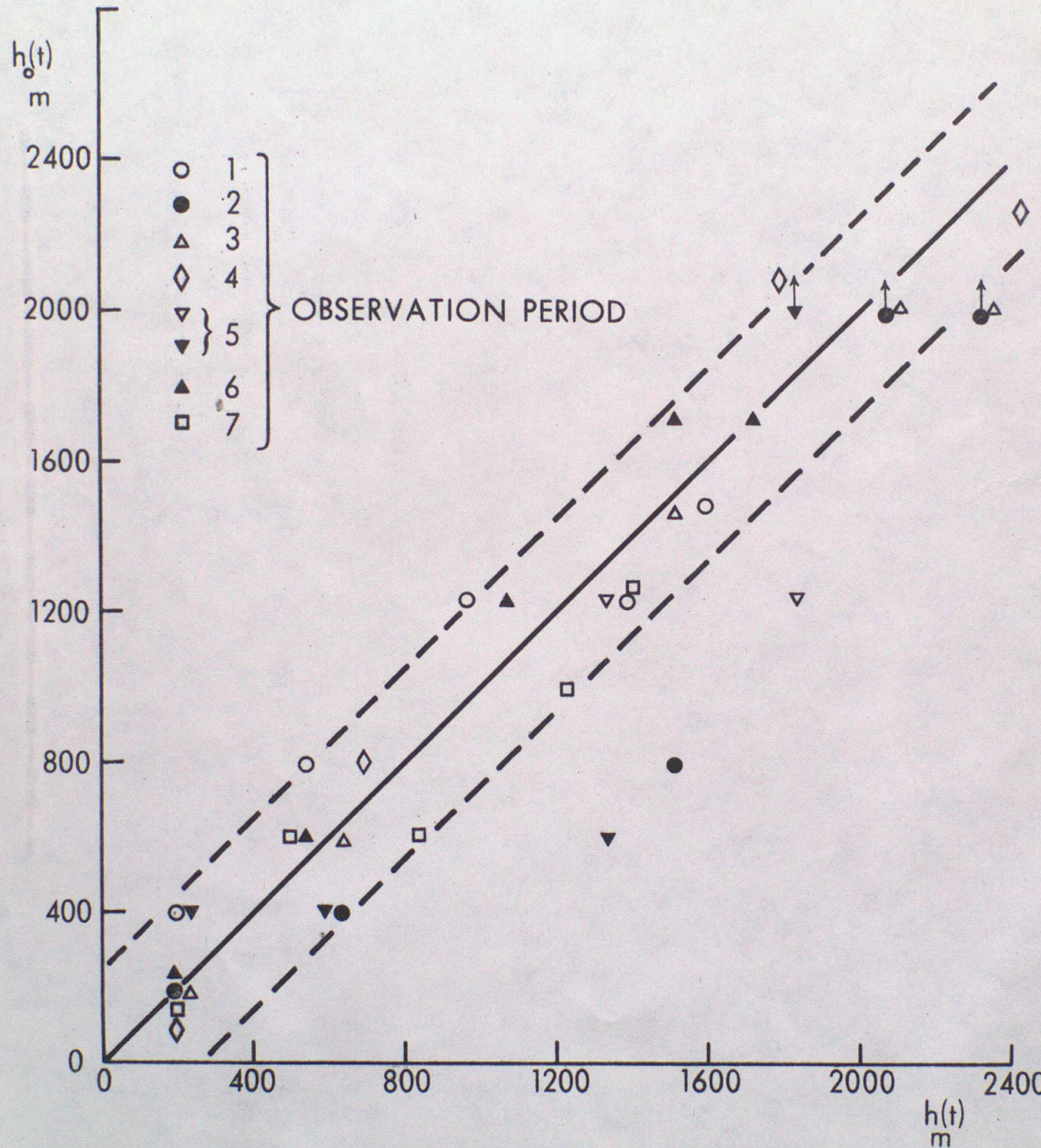

Figure 13. The depth of the O'Neill boundary layer, $h_o(t)$, estimated from profiles, against the depth, $h(t)$, predicted using a three-phase model. The broken lines are $h_o(t) = h(t) \pm 255$ m, where 255 m is the standard error about the line $h_o(t) = h(t)$, the correlation coefficient being 0·93.